IEEE Access
Multidisciplinary | Rapid Review | Open Access Journal

Received December 11, 2020, accepted December 26, 2020, date of publication January 1, 2021, date of current version January 12, 2021.

Digital Object Identifier 10.1109/ACCESS.2020.3048781

High-Power Lensless THz Imaging of Hidden Objects

SAMIRA MANSOURZADEH[1], DILYAN DAMYANOV[2], TIM VOGEL[1], FRANK WULF[1], ROBERT B. KOHLHAAS[3], BJÖRN GLOBISCH[3,4], THORSTEN SCHULTZE[2], MARTIN HOFFMANN[1], JAN C. BALZER[2], AND CLARA J. SARACENO[1]

[1]Photonics and Ultrafast Laser Science, Ruhr Universität Bochum, 44801 Bochum, Germany
[2]Chair of Communication Systems, University of Duisburg–Essen, 47057 Duisburg, Germany
[3]Fraunhofer Institute for Telecommunications, Heinrich Hertz Institute (HHI), 10587 Berlin, Germany
[4]Department of Solid State Physics, Technische Universität Berlin, 10623 Berlin, Germany

Corresponding author: Samira Mansourzadeh (mansourzadeh.samira@ruhr-uni-bochum.de)

This work was supported in part by the Deutsche Forschungsgemeinschaft (DFG, German Research Foundation) under Project 287022738 TRR 196 and Project C10 and M05, in part by the Germany's Excellence Strategy – EXC-2033 – Projektnummer 390677874 - RESOLV, and in part by the Alexander von Humboldt Stiftung (Sofja Kovalevskaja Preis). We acknowledge support by the DFG Open Access Publication Funds of the Ruhr-Universität Bochum.

ABSTRACT The potential of pulsed THz radiation for time-of-flight imaging applications is well recognized. However, advances in this field are currently severely limited by the low average power of ultrafast THz sources. Typically, this results in impractically long acquisition times and a loss in resolution and contrast. These limitations make imaging of the objects in real-life scenarios impossible. Here, conclusively, the potential of state-of-the-art high-average power THz time-domain spectrometer (TDS), driven by a 100-W class, one-box ultrafast oscillator for imaging applications is shown by demonstrating lensless THz imaging in reflection mode of a dielectric sample with low reflectivity. Images obtained with our home-built 20-mW average power THz-TDS system show a significant contrast enhancement compared to a state-of-the-art commercial THz-TDS with less than 200 μW of average power. Our unique setup even allows us to obtain images of such an object with high-contrast hidden inside a medium-density fiberboard (MDF) box. This opens the door to THz time-of-flight imaging of concealed objects of unknown shape and orientation in various real-life scenarios which were so far impossible to realize.

INDEX TERMS High-power terahertz radiation, lensless terahertz imaging, terahertz time-domain spectroscopy.

I. INTRODUCTION

Terahertz (THz) radiation is well-known to have enormous potential for imaging in various fields such as security [1], non-destructive testing [2], biomedical research [3], as well as in fundamental research applications such as nanoscale imaging in a condensed matter [4]. In applied fields such as security and testing, electromagnetic waves in the THz domain have the advantage that they are able to penetrate deep into materials which are usually opaque at visible and infrared wavelengths [5], [6] opening the door to imaging and characterizing material properties of concealed objects. Compared to more classically used microwave systems, THz radiation enables us to achieve significantly higher resolution [7].

However, widespread use of THz imaging in real-life scenarios remains limited, mostly due to the low average power of commercial THz sources. In fact, a realistic imaging scenario is typically in a reflection geometry with low reflectivity materials, where the beam gets reflected off the sample and propagates to the detector. Objects of our daily life exhibit complex diffraction and scattering effects, where the roughness becomes comparable to the illumination wavelength and make it especially challenging to create a high contrast THz image. Therefore, minuscule amounts of radiation reach the corresponding detectors, thus calling for high illumination power in combination with high detection sensitivity. In this respect, THz time-domain spectroscopy (THz-TDS) offers the advantage of highly sensitive field-resolved detection [8], particularly based on optimized photoconductive antennas [9]. However, THz-TDS particularly suffers from a severe lack of high-average power, with typical sources in the

The associate editor coordinating the review of this manuscript and approving it for publication was Ravibabu Mulaveesala.

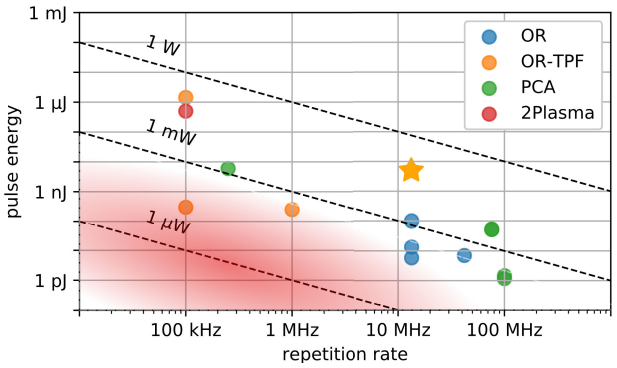

FIGURE 1. State-of-the-art of lab-based THz-TDS sources with more than 100 kHz of repetition rate, as required for imaging applications. The typical operation range of THz-TDS systems (<100 μW of THz average power) is marked with a red background. OR: optical rectification, OR-TPF: optical rectification-tilted pulse front, PCA: photoconductive antenna, 2Plasma: Two-color ionized gas plasma. The yellow star highlights the last power record value from our group presented in [20].

microwatt regime (Fig. 1), severely limiting progress in this field.

In this article, we demonstrate that state-of-the-art high-average power THz-TDS with tens of milliwatts of average power are groundbreaking tools for THz imaging applications and promise to open up this field.

To date, numerous imaging setups have been introduced using THz-TDS, mostly exploiting time-of-flight techniques [10], whereby the temporal delay between reflected THz pulses imparts the internal structure of the sample [11]. This technique has been extensively exploited to analyze the layer structure of materials (for example, a Putto, which is a wood carving of an infant), was analyzed by THz-tomography in [12] or in the biomedical field for histopathological imaging of cancerous tissue [13]. Another prominent application is hidden object detection in security applications [14] which have been demonstrated, albeit only looking through thin, low-THz-absorption test materials [15], [16].

Nevertheless, several difficulties have hindered THz time-of-flight imaging to become widespread, particularly in the above-mentioned real-life scenarios. Typically, lenses or off-axis parabolic mirrors are used to collimate the THz beam and re-focus it onto the sample under test. For detection, the reflected beam has to be guided to the detector with additional optical elements, which results in two major difficulties: A precise alignment requires prior information about the position, orientation, and shape of the sample, which are usually unknown in real-life scenarios. Second, the frequency dependent spot size limits the lateral resolution and therefore, a tight focusing is only achieved for limited depth of field. An approach to mitigate the challenge of arbitrarily shaped surfaces is based on a multistage robotic arm procedure: at first the surface shape of the object under test is captured by a structured light scanner, then a trajectory for the robotic arm is calculated which ensures that the surface of the object is always perpendicular to the incident radiation and in the focal point, and finally the imaging in the THz domain itself is performed [17]. Although this approach was successfully used to image the inner structure of ancient human remains [18], the alignment of the system is restricted to the contour map of the sample under test. If an object contains hidden or internal surfaces, which are not parallel to the contour map, imaging is not possible. Further, the limited depth of field of a focused system distorts the image when the object is significantly thicker than the Rayleigh length of the focused beam.

A promising method to overcome these difficulties has been introduced and evaluated by Damyanov *et al.* [19]. The proposed imaging configuration is a lensless scheme, which is a migration-based radar image reconstruction. In this scheme, when a divergent THz beam is used for reflection-mode imaging, every section of the sample is illuminated under a different angle. If the emitter and the detector move with respect to the sample, the contributions from different parts of the sample change. The reflected beam from each part of the sample surface provides plenty of information to explore sample size and shape. The reflected beam from interfaces with different refractive indices provide information about inner structure. All information is contained in a two-dimensional dataset, which is known as a radargram in the mm-wave community, that depicts the detected signal in time-domain as a function of the relative position between emitter, sample, and detector. The image of an object can be reconstructed by using the time-of-flight information of the radargram and the knowledge of the position of the THz detector and emitter in each measurement. The main advantage of this procedure is that the image is retrieved from the complete time-domain data, and no a priori information about the position or shape of the object is required. An additional advantage when compared to lens-based imaging is the use of a synthetic aperture for image reconstruction: the focusing of the divergent THz beam is achieved in the post-processing step and not by optical elements. Hence, this algorithm can be employed for imaging without focusing optics or prior knowledge about the properties of the sample, which makes it extremely attractive for real-world applications.

However, the most critical difficulty in this technique is that illumination is done with a typically low-average power divergent THz beam, resulting in minimal reflected signal strength at the receiver and minuscule signal-to-noise ratio (SNR) figures, limiting the imaging capabilities especially for the through-wall detection/imaging of structured subsurface samples with high THz absorption through an obstacle and at long distance. Further, nonpolar and nonmetallic materials usually have high transmission loss, making imaging through typical obstacles, i.e., wood, glass, and stone, challenging.

For this and other applications, many groups worldwide have recently started to explore the possibilities opened by novel high-average power ultrafast lasers with hundreds of watts of average power to increase the average power of THz-TDS, resulting in significant advances [20]–[22]; reaching nowadays a performance level which was traditionally only achieved with accelerator-based sources [23], see Fig. 1.

For the targeted imaging applications, we focus our attention on systems with high repetition rate much greater than 1 MHz because of the otherwise extremely long acquisition time. The lack of high average power THz-TDS sources is particularly severe in this high repetition rate regime. In this respect, one high-average power ultrafast laser technology stands out as particularly promising, namely modelocked thin-disk laser (TDL) oscillators, to drive THz generation [24]. These one-box modelocked oscillators operate at MHz repetition rates but outperform other oscillator technologies by several orders of magnitude in terms of average power [20], [25], providing the same output power levels as complex multi-chain amplifiers with additional advantages such as potentially low-noise levels close to the quantum limit of high-Q resonator [26] and transform-limited femtosecond pulses. The state-of-the-art of these oscillators is 350 W average power with pulse duration of 940 fs, and a repetition rate of 8.88 MHz [27], and 80-μJ pulse energy at 242 W of average power [28]. Based on this technology, we recently achieved a THz-TDS with 66 mW of average power, based on optical rectification in the tilted pulse front regime in Lithium Niobate (LN), which is the highest average power reported so far from a single-cycle THz source at multi-MHz repetition rates [20]. However, so far, the potential of this and other unique high-average power THz-TDS sources for high-dynamic range applications had not been conclusively demonstrated.

In this article, we demonstrate that state-of-the-art high-average power THz-TDS are groundbreaking tools for THz imaging applications and promise to open up this field. Using our record-high average power 20-mW class THz-TDS, we perform lensless time-of-flight imaging in reflection mode of a 3D-printed mixed polymer sample in several configurations, showing on the one hand a significant contrast enhancement compared to a commercial THz-TDS system, and on the other hand excellent image reconstruction even when the object is hidden inside a box made of a highly absorptive THz material (in this case medium-density fiberboard, MDF) with a total attenuation of 6.7 dB). To the best of our knowledge, this is the first time that THz imaging of a concealed, low-reflective sample with an unknown position and shape is demonstrated. These results open the door to new advances in THz imaging and sensing based on high average power THz-TDS.

II. EXPERIMENTAL SETUP

The experimental setup is shown in Fig. 2. The femtosecond laser system used to drive THz generation in LN is a home-built modelocked thin-disk oscillator based on Yb:LuAG. It is operating in the soliton modelocking regime [28], [29], using a semiconductor saturable absorber mirror (SESAM) [31] for starting and stabilization of the soliton-shaped pulses. The laser system as used in this specific experiment has the same layout as the laser in [20]. It delivers up to 100 W of average power at 13.4-MHz repetition rate, corresponding to 7.5-μJ pulse energy. The pulse duration at this average power

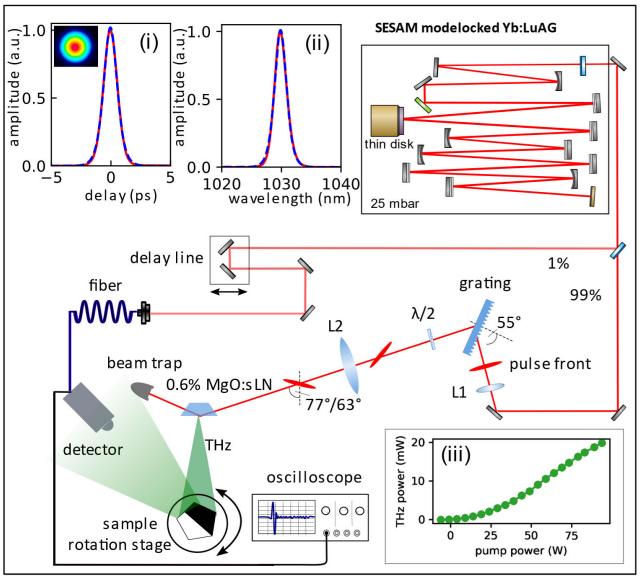

FIGURE 2. Experimental setup, driving laser and high average-power THz-TDS with lensless imaging setup: The sample illuminated by a diverging THz beam is placed on top of a rotation stage, a PCA is placed in front of the sample to detect the reflected beam. The top-left insets show the oscillator characteristics: (i), autocorrelation trace with sech^2-fit and the inset shows the laser beam profile. (ii): laser spectrum with sech^2-fit. The inset (iii) shows the THz average power vs. laser pump power.

is 550 fs. The central wavelength of the laser is 1030 nm. It is worth noting that contrarily to many amplifier technologies capable of this performance level, our oscillator delivers transform-limited, clean sech^2-shaped pulses and diffraction-limited beam quality, inherent to TDLs. The excellent temporal and spectral quality of the laser is illustrated in Fig. 2, in the inset (i) and (ii). To demonstrate the reliability of the laser, a long-term power stability measurement with a thermopile powermeter was performed. An average power of 107.5 W with an excellent root mean square (RMS) value of 0.15% over 17 hours was measured. Moreover, we analyzed the high-frequency noise of the laser using a fast photodiode and a microwave signal analyzer (Rohde & Schwartz FSWP50). The relative intensity noise of better than 0.1% was calculated in the frequency range from 10 Hz to 10 MHz [32].

The high-power oscillator is used to directly drive THz generation in a MgO-doped stoichiometric trapezoid LN crystal with a pulse front tilt of 63° to achieve velocity matching, in a similar layout to [20]. A transmission grating with an angle of incidence of 54.5° (Littrow angle) is imaged to the LN crystal using an aspherical lens with a focal length of 87 mm to tilt the pulse front of the laser [20]. The generated THz beam is emitted perpendicularly to the front surface of the trapezoid. To measure the THz average power, a calibrated thermopile detector is employed. In this configuration, we routinely generate THz radiation with average powers up to 20 mW, which are then used for the imaging experiments. We note that here that higher average powers are possible to achieve with shorter driving pulses as shown in [20]. However, in the imaging experiment we aimed for the simplest possible setup (oscillator driven, without external

pulse compression modules). For full THz field reconstruction, we use a fiber-coupled photoconductive antenna (PCA) from Fraunhofer Heinrich-Hertz-Institute, Berlin, Germany based on an InAlAs/InGaAs heterostructure [33]. A 1-m single-mode, polarization-maintaining fiber is attached to the module to direct the probe laser beam to the antenna. To focus the incoming pulses, the receiver antenna is mounted on a hyper-hemispherical high-resistivity float-zone silicon lens with 10 mm diameter. The antenna has been designed to operate at a wavelength of 1550 nm. However, it can also be operated with a 1030-nm probe with comparable dispersion properties. It is worth highlighting that the probe beam has a long pulse duration, thus is not significantly affected by dispersion at this fiber length. In the experiment, the probe power coupled into the antenna is 5 mW. The output of the antenna is connected to a low noise transimpedance amplifier with switchable gain up to 1×10^8 V/A and bandwidth up to 200 MHz. In order to create the delay between pump and probe arm in the setup, two options are available: a shaker for fast scanning and live visualization of the THz trace and a linear stage in combination with lock-in detection, which we use depending on the requirements of each specific setup presented below. First, a comparison experiment between our setup and a commercial THz-TDS from Menlo Systems GmbH is shown in section III.A and III.B. To have a fair comparison, we were using a shaker like their method as a delay line. The shaker in our setup has a scanning frequency of 1.5 Hz and a travel range of 50 mm, which corresponds to 330 ps of time delay. This total temporal range results in a frequency resolution of 3.03 GHz in the frequency domain. However, to be able to detect the weak signal in the concealed object experiment in the section III.C, a linear stage with lock-in amplifier detection is implemented.

In the imaging setup, the object to be imaged is illuminated by the divergent beam and placed on a rotation stage to get a full 2D rotational scan with the detector placed at a fixed angle in reflection where only a minuscule amount of the back-reflected power reaches the PCA. For benchmarking the performance of our unique high-power THz-TDS system, we also use a state-of -the-art commercial THz-TDS system (Tera-K15, Menlo Systems) in the same geometrical configuration. This setup uses a driving laser with 20 mW of average power, 80 fs pulses at 100-MHz repetition rate. The emitted THz power is less than 200 μJ.

In imaging experiments using a synthetic aperture radar approach, usually emitter and detector are moved around the sample under test in our setup, the emitter and detector remain static and the sample is rotated to simplify the experimental layout, which does not change the principles of the imaging technique (known as inverse synthetic aperture radar approach). The image is reconstructed from the THz time-domain traces at each rotation step, as explained in the previous section. In both experiments, the distance from the LN crystal to the sample is 0.25 m and from the sample back to the PCA detector 0.22 m.

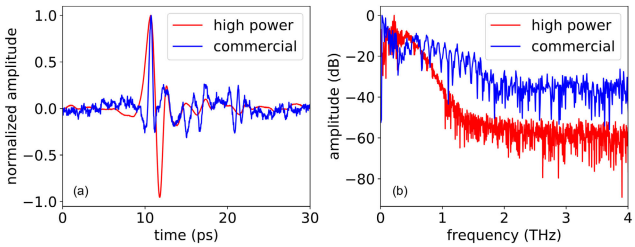

FIGURE 3. Comparison of high-power THz-TDS (red) and commercial low power THz-TDS (blue) using the reflected THz beam from a metal beam block (a) time trace, (b) frequency domain.

III. RESULTS

In the following, three experiments to demonstrate the capabilities of our imaging system are presented. First, measurements using an ideal reflector, here a metal plate, are performed with both systems to analyze the dynamic range of a single THz trace. Then 360° circular scans of a sample under test are performed to get 2D image with high-power and commercial THz-TDS systems to compare the imaging capabilities of both systems. Finally, a similar circular scan is done only with the high-power system, but with the object inside an MDF box for the demonstration of through-wall lensless THz imaging.

A. BENCHMARKING OF HIGH-POWER AND COMMERCIAL THZ-TDS

In order to benchmark the performance of our high-power THz-TDS in terms of dynamic range, we measure the reflected THz beam from a 200 m $\times$ 75 mm flat metallic plate (anodized bead-blasted aluminum) placed at the position of the object we want to image. Measurements are performed using both, the high-power THz-TDS and the commercial THz-TDS from Menlo Systems described in detail above. The metallic plate provides an ideal reflection without any influence of the targe's physical properties, such as shape, size, or material characteristics. It is worth noting here that it is not possible to calibrate the PCA response used for detection using the full power of our THz source by focusing on it, as these are designed for high sensitivity at low THz power, and exhibit saturation at high driving THz power. Antenna designs capable of supporting high-average power levels are currently being separately investigated but are out of the scope of this article.

Fig. 3 shows the signal reflected from a metallic plate. Random noise in the measurement can be reduced by averaging a series of traces in the time domain obtained from multiple repetitive measurements [34]. The illustrated signals in Fig.3 are averaged over 40 traces in the time domain for both TDS systems. We used the same detector for both systems and an identical location for emitter and detector. It is worth noting that the two setups have slightly different divergence angles, 25° in the commercial setup and around 30° for the high-power source. Using both THz-TDS, the diverging beam has a diameter of approximately 10 cm at the position of the sample, larger than the size of the sample. One part of the

beam covers the sample, but the other part of the beam just passes by the sample and does not get reflected. This results in an additional loss – increasing the requirements in terms of illumination power. We do not correct the position of the object, as we focus our attention on comparing the setups in an identical imaging scenario. Nevertheless, it is clear that at a fixed distance, this will be a disadvantage for our high-power setup, and potentially even better results can be obtained by optimizing the object distance. In Fig 3.a, the time-trace of the pulses averaged over 40 traces is shown. The generated pulse duration is shorter in the commercial setup than in our home-built one, due to the shorter driving pulses. However, comparing the time-domain form of two pulses, the detected pulse from the high-power system exhibits a clear single-cycle pulse with low noise components, whereas the pulse detected with the state-of-the-art commercial system exhibits strong artifacts and stronger noise components. The corresponding spectrum of the averaged pulses is illustrated in Fig 3.b reaching 2 THz for the commercial setup (within the detected dynamic range), and around 1 THz for our high-power setup. The frequency-domain dynamic range using high THz power is improved by more than 20 dB, compared to the commercial system, illustrating the advantage of the setup for the targeted application. It should be noted however, that the shorter pulses in the commercial setup should be advantageous for the imaging experiment due to the higher resolution depth reachable with shorter pulses. Nevertheless, the high-average power source outperforms the commercial system in terms of image quality as we will see in the following section, indicating the potential of this source for through-wall imaging application and already setting possible improvements for future developments of our high-average power THz-TDS. For example, the high dynamic range allows the application of replica waveforms with a higher bandwidth to increase the axial image resolution significantly [35].

B. IMAGING USING HIGH-POWER AND COMMERCIAL THZ-TDS

Our imaging sample is a 3D printed pentagonal-shape mixed polymer sample, which includes two types of polymers: the black part is tough Polylactide (PLA), and the white part is Polypropylene (PP). The top view picture of the sample and optical properties of the 3D printed polymers in the THz regime [36] are given in Fig. 4. Due to the low refractive index of PLA and PP, the reflectivity is very low, which explains why such objects are typically difficult to image in such a setup.

The imaging method is designed to work for samples of unknown orientation and position, therefore no a priori information about the position of the sample is required [19]. Measurements are performed continuously during a full 360° rotation of the polymer sample in steps of 1° with 20 trace averages per step. A high-resolution 10-bit oscilloscope with a sampling rate of 200 kSample/s is used for data acquisition. For the realization of the measurements, delay lines/shakers with equal travel range were considered for both setups. As

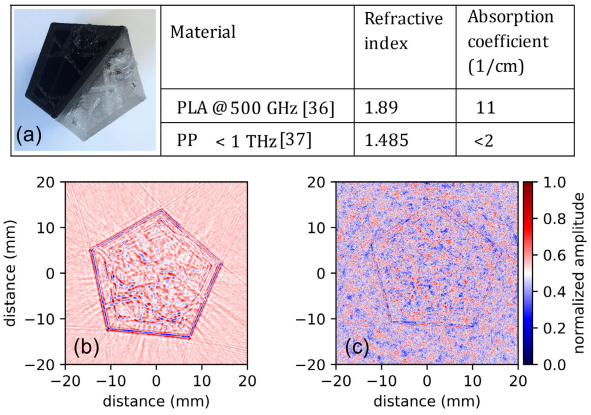

FIGURE 4. (a) 3D printed sample top-view and materials specification in the THz regime [36], [37]. Retrieved image of the pentagonal object, (b) using our high-power homebuilt THz setup and (c) Menlo System TDS setup. For each image, the result is independently normalized to their maximum value.

it was mentioned before, the shaker has a scanning frequency of 1.5 Hz and a travel range of 50 mm which can cover the time delay caused by the reflection on the pentagonal sample with an edge length of 18 mm. We imaged the same object with the commercial system and the high-power setup using the same number of the averaged traces, the same integration time, and the same antenna configuration.

The resulting images from both systems are shown in Fig. 4. The x and y-axis indicate the position of the sample, and the z-axis shows the normalized reconstructed amplitude from the measured data. It should be mentioned that for each image, the result is independently normalized to their maximum value.

The figures demonstrate the enhanced imaging capability of the high-power system. The contour of the target is reconstructed clearly with very low residual noise, whereas in the case of the commercial system, the target is nearly lost in the noise level. Furthermore, since the THz beam can partially penetrate through the 3D printed sample and the 3D printer does not fill the sample completely, the cavities in the sample can lead to the imaged structure. This inner structure of the sample is only visible with the high-power system, and one can recognize that the object is made of two different materials. The total time to image the sample with the high-power source was less than 2 hours and with the commercial setup around 1 hour. The mismatch between imaging time in both systems was only caused by the limited data transfer rate from the oscilloscope.

To quantify the quality of the images and prove the enhancement in image quality using the high-power system, a no-reference image quality assessment called Perception-based Image Quality Evaluator (PIQUE) is employed [38]. This technique extracts the local features to predict the quality of the image, and it does not require any training data. The quality scale of the image based on this method is from 0 to 100: the PIQUE score between 0 to 30 represents a good quality image, between 50 to 100 refers to a poor-quality

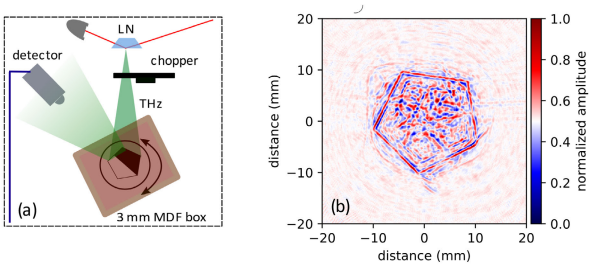

FIGURE 5. Imaging of the 3D printed polymer pentagonal sample inside a 3-mm thick MDF box, (a) modified imaging setup, (b) retrieved image of the sample, the data was acquired by a lock-in amplifier. The sample has an edge length of 12 mm.

image, and any value between 30 to 50 can be treated as a fair quality image. The calculated PIQUE score for the two images shown in Fig. 4 is 23.9 out of 100 and 73.6 out of 100 for the high-power and commercial setup, respectively. As expected from this evaluation, the image reconstructed with the data from the high-power system has a much lower score, which indicates its higher quality in comparison to the commercial one. To prove the robustness of the algorithm, images acquired in different displaying circumstances are used: different colormaps and different pixel value scaling, resulted in similar scores. Another possibility to quantify the contrast of the reconstructed image from both systems is to calculate the dynamic range of both images by comparing the noise level of the image with a maximum pixel value. To calculate the noise floor, we take a 5 mm $\times$ 5 mm area next to the object, and afterward, the average intensity of the top 5%-pixel values is divided by the noise floor. The calculated values for the high-power and the commercial system are 1899 and 514, respectively, showing the considerable enhancement in image contrast for the high-power system.

C. IMAGING THE SAMPLE PLACED IN AN MDF BOX

In this section, we target to explore the limits of our high-power setup for lensless imaging by imaging a similar low reflectivity polymer object in the same reflection configuration, only this time hidden inside a box. The modified setup is shown in Fig. 5. For the box material, MDF material with 3-mm thickness is used. It should be mentioned that in a real through-wall imaging scenario, the box would be moving too with the sample, but in our experiment, it is stationary to simulate a lossy path and simplify the setup. The loss of this material was characterized using our THz-TDS in transmission mode, measuring -3.35 dB for one pass, resulting in a total additional loss of 6.7 dB in our specific experimental setup. Unfortunately, after the first experiment, the exact sample was not available to us anymore for the second part. Therefore, we 3D printed a new sample made of the same polymers as the first sample. It has the same pentagonal shape as our first experiment but with a different edge size of 12 mm. The configuration and all distances between crystal, sample and PCA detector are the same as in the previous experiment. For this extreme case with additional THz attenuation and in order to explore the limits of our setup, we use the more sensitive lock-in detection with a motorized stage at the expense of a longer measurement time. The output of the transimpedance amplifier is connected to the lock-in amplifier synchronized with an optical chopper (set at a frequency of 627 Hz) to acquire the PCA responses. Measurements are performed during a full 360° rotation of the sample in steps of 2°. The motion of the rotation stage is in steps and the data is acquired not continuously but point by point in each step of the rotation stage. In each measurement, the reflected THz beam from the sample is probed with a translation stage with the step-and-settle, non-continuous sampling strategy. The stage moves step by step, and in every step, the lock-in amplifier records the signal value received from the PCA with a time constant of 10 ms. The number of the steps is 1024, which corresponds to a step size of 195 fs. When a full trace with 1024 points is acquired, the linear stage move to its starting position and the rotation stage was moved 2° further. After the rotation stage is stationary, the next trace is recorded.

The reconstructed image of the sample is computed employing the same algorithm presented in the previous sections, illustrated in Fig. 5.b. The shape of the object is retrieved with a clear contour, and the size of it is perfectly matched with the measured edge length of 12 mm. To quantify the image quality, the PIQUE method mentioned previously is used. The calculated score is 20.3, which indicates a high quality of the image. The PIQUE score here with the box is less than the value calculated for the image with the shaker (23.9), although there is higher attenuation than before due to the MDF box. This shows the advantage of using a linear stage with lock-in to detect the low-strength signal. However, this comes at the expense of a much longer measurement time – which was in our setup 10 hours and increases the sensitivity of our setup to slowly varying environmental fluctuations such as temperatures changes and slow drifts of the laser system. Below, the future improvements will be discussed that can be realized in our setup to consider imaging in such difficult scenarios with much shorter measurement times.

IV. CONCLUSION

In summary, we demonstrated the potential of state-of-the-art high-average power THz-TDS for THz imaging applications by performing lensless imaging of a 3D-printed mixed polymer object using a migration algorithm, which can reconstruct the image of the object without liming us to have a priori information about the shape and position of the object. Images obtained with our 20-mW average power THz-TDS shows a clear enhancement of dynamic range, which results in a significantly improved image contrast compared to the same measurements performed using a state-of-the-art commercial TDS system with less than 200 μW of average power. Furthermore, we have demonstrated through-wall lensless imaging with the test object concealed in an MDF box using our source. To the best of our knowledge, this represents the first application that conclusively shows the immense potential of high-average power, high-repetition

rate THz sources by achieving extremely clear images of a low-reflectivity probe inside a box with considerable THz absorption, which had so far not been realized.

It is worth noting that although we did not target an identification of the material of the dielectric object in this first experiment, THz-TDS traces have potential to extract material signatures that can also be exploited to identify the material, for example using machine learning algorithms – a direction we plan to explore in the future.

It is also worth highlighting here that these results were achieved in spite of several flaws in the setup: the antenna was not designed for 1030-nm wavelength resulting in reduced responsivity, the repetition rate was an order of magnitude lower than typically used in low-power THz-TDS systems, and our pulse duration was approximately 5 times longer than in the commercial setup, resulting in a lower resolution depth for the image reconstruction. Nevertheless, the quality of the images exceeds the capabilities of the low-average power setup. This is a decisive demonstration of the potential of such novel high-average power sources for imaging applications. In the near future, we plan to optimize our setup using an adapted laser system with shorter excitation pulses, scale the repetition rate to higher values to enable shaker detection even in the most difficult scenarios, and develop optimized antennas for our wavelength region to further enhance sensitivity. This will allow us to image objects in even more difficult scenarios (hidden in walls for example) at higher speed and even to fully reconstruct the object in 3D.

REFERENCES

[1] J. F. Federici, B. Schulkin, F. Huang, D. Gary, R. Barat, F. Oliveira, and D. Zimdars, "THz imaging and sensing for security applications—Explosives, weapons and drugs," *Semicond. Sci. Technol.*, vol. 20, no. 7, pp. S266–S280, Jun. 2005, doi: 10.1088/0268-1242/20/7/018.

[2] I. Amenabar, F. Lopez, and A. Mendikute, "In introductory review to THz non-destructive testing of composite mater," *J. Infr., Millim., THz Waves*, vol. 34, no. 2, pp. 152–169, Feb. 2013, doi: 10.1007/s10762-012-9949-z.

[3] U. R. Pfeiffer, T. Zimmer, P. Hillger, R. Jain, J. Grzyb, T. Bucher, Q. Cassar, G. MacGrogan, J.-P. Guillet, and P. Mounaix, "*Ex vivo* breast tumor identification: Advances toward a silicon-based terahertz near-field imaging sensor," *IEEE Microw. Mag.*, vol. 20, no. 9, pp. 32–46, Sep. 2019, doi: 10.1109/MMM.2019.2922119.

[4] H. T. Stinson, A. Sternbach, O. Najera, R. Jing, A. S. Mcleod, T. V. Slusar, A. Mueller, L. Anderegg, H. T. Kim, M. Rozenberg, and D. N. Basov, "Imaging the nanoscale phase separation in vanadium dioxide thin films at terahertz frequencies," *Nature Commun.*, vol. 9, no. 1, p. 3604, Dec. 2018, doi: 10.1038/s41467-018-05998-5.

[5] Y.-S. Lee, *Principles of Terahertz Science and Technology*. Boston, MA, USA: Springer, 2009.

[6] P. Dean, A. Valavanis, J. Keeley, K. Bertling, Y. L. Lim, R. Alhathlool, A. D. Burnett, L. H. Li, S. P. Khanna, D. Indjin, T. Taimre, A. D. Rakić, E. H. Linfield, and A. G. Davies, "Terahertz imaging using quantum cascade lasers—A review of systems and applications," *J. Phys. D, Appl. Phys.*, vol. 47, no. 37, Sep. 2014, Art. no. 374008, doi: 10.1088/0022-3727/47/37/374008.

[7] D. M. Mittleman, "Twenty years of terahertz imaging [invited]," *Opt. Exp.*, vol. 26, no. 8, p. 9417, Apr. 2018, doi: 10.1364/OE.26.009417.

[8] L. Valzania, Y. Zhao, L. Rong, D. Wang, M. Georges, E. Hack, and P. Zolliker, "THz coherent lensless imaging," *Appl. Opt.*, vol. 58, no. 34, pp. G256–G275, Dec. 2019, doi: 10.1364/AO.58.00G256.

[9] R. B. Kohlhaas, S. Breuer, S. Nellen, L. Liebermeister, M. Schell, M. P. Semtsiv, W. T. Masselink, and B. Globisch, "Photoconductive terahertz detectors with 105 dB peak dynamic range made of rhodium doped InGaAs," *Appl. Phys. Lett.*, vol. 114, no. 22, Jun. 2019, Art. no. 221103, doi: 10.1063/1.5095714.

[10] E. Bründermann, H.-W. Hübers, and M. F. Kimmitt, *Terahertz Techniques*. Berlin, Germany: Springer-Verlag, 2012.

[11] H. Guerboukha, K. Nallappan, and M. Skorobogatiy, "Toward real-time terahertz imaging," *Adv. Opt. Photon.*, vol. 10, no. 4, pp. 843–938, Dec. 2018, doi: 10.1364/AOP.10.000843.

[12] E.-M. Stubling, N.-A. Staats, B. Globisch, M. Schell, H. D. Portsteffen, and M. Koch, "Investigating the layer structure and insect tunneling on a wooden putto using robotic-based THz tomography," *IEEE Trans. THz Sci. Technol.*, vol. 10, no. 4, pp. 343–347, Jul. 2020, doi: 10.1109/TTHZ.2020.2986652.

[13] A. D'Arco, M. D. Di Fabrizio, V. Dolci, M. Petrarca, and S. Lupi, "THz pulsed imaging in biomedical applications," *Condens. Matter*, vol. 5, no. 2, p. 25, Apr. 2020, doi: 10.3390/condmat5020025.

[14] W. R. Tribe, D. A. Newnham, P. F. Taday, and M. C. Kemp, "Hidden object detection: Security applications of terahertz technology," *Proc. SPIE*, vol. 5354, p. 168, Apr. 2004, doi: 10.1117/12.543049.

[15] M. Kowalski, "Hidden object detection and recognition in passive terahertz and mid-wavelength infrared," *J. Infr., Millim., THz Waves*, vol. 40, nos. 11–12, pp. 1074–1091, Dec. 2019, doi: 10.1007/s10762-019-00628-7.

[16] Z. Ou, J. Wu, H. Geng, X. Deng, and X. Zheng, "Confocal terahertz SAR imaging of hidden objects through rough-surface scattering," *Opt. Exp.*, vol. 28, no. 8, p. 12405, Apr. 2020, doi: 10.1364/OE.388392.

[17] E. Stübling, Y. Bauckhage, E. Jelli, B. Fischer, B. Globisch, M. Schell, A. Heinrich, J. C. Balzer, and M. Koch, "A THz tomography system for arbitrarily shaped samples," *J. Infr., Millim., THz Waves*, vol. 38, no. 10, pp. 1179–1182, Oct. 2017, doi: 10.1007/s10762-017-0415-9.

[18] E.-M. Stübling, A. Rehn, T. Siebrecht, Y. Bauckhage, L. Öhrström, P. Eppenberger, J. C. Balzer, F. Rühli, and M. Koch, "Application of a robotic THz imaging system for sub-surface analysis of ancient human remains," *Sci. Rep.*, vol. 9, no. 1, Dec. 2019, Art. no. 3390, doi: 10.1038/s41598-019-40211-7.

[19] D. Damyanov, I. Willms, J. C. Balzer, B. Friederich, M. Yahyapour, N. Vieweg, A. Deninger, K. Kolpatzeck, X. Liu, A. Czylwik, and T. Schultze, "High resolution lensless terahertz imaging and ranging," *IEEE Access*, vol. 7, pp. 147704–147712, 2019, doi: 10.1109/ACCESS.2019.2934582.

[20] F. Meyer, T. Vogel, S. Ahmed, and C. J. Saraceno, "Single-cycle, MHz repetition rate THz source with 66 mW of average power," *Opt. Lett.*, vol. 45, no. 9, p. 2494, May 2020, doi: 10.1364/OL.386305.

[21] J. Buldt, M. Mueller, H. Stark, C. Jauregui, and J. Limpert, "Fiber laser-driven gas plasma-based generation of THz radiation with 50-mW average power," *Appl. Phys. B, Lasers Opt.*, vol. 126, no. 1, p. 2, Jan. 2020, doi: 10.1007/s00340-019-7353-2.

[22] P. Kramer, M. C. Hoffmann, and F. Tavella, "Generation of high-field single-cycle terahertz pulses at 100 kHz," in *Proc. Conf. Lasers Electro-Optics*, May 2020, pp. 1–2, Paper STu3G.4.

[23] E. Chiadroni *et al.*, "The SPARC linear accelerator based terahertz source," *Appl. Phys. Lett.*, vol. 102, no. 9, Mar. 2013, Art. no. 094101, doi: 10.1063/1.4794014.

[24] C. J. Saraceno, D. Sutter, T. Metzger, and M. A. Ahmed, "The amazing progress of high-power ultrafast thin-disk lasers," *J. Eur. Opt. Soc.-Rapid Publications*, vol. 15, no. 1, p. 15, Dec. 2019, doi: 10.1186/s41476-019-0108-1.

[25] F. Meyer, N. Hekmat, T. Vogel, A. Omar, S. Mansourzadeh, F. Fobbe, M. Hoffmann, Y. Wang, and C. J. Saraceno, "Milliwatt-class broadband THz source driven by a 112 W, sub-100 fs thin-disk laser," *Opt. Exp.*, vol. 27, no. 21, pp. 30340–30349, Oct. 2019, doi: 10.1364/OE.27.030340.

[26] F. Emaury, A. Diebold, C. J. Saraceno, and U. Keller, "Compact extreme ultraviolet source at megahertz pulse repetition rate with a low-noise ultrafast thin-disk laser oscillator," *Optica*, vol. 2, no. 11, pp. 980–984, Nov. 2015, doi: 10.1364/OPTICA.2.000980.

[27] F. Saltarelli, I. J. Graumann, L. Lang, D. Bauer, C. R. Phillips, and U. Keller, "Power scaling of ultrafast oscillators: 350-W average-power sub-picosecond thin-disk laser," *Opt. Exp.*, vol. 27, no. 22, pp. 31465–31474, Oct. 2019, doi: 10.1364/OE.27.031465.

[28] C. J. Saraceno, F. Emaury, C. Schriber, M. Hoffmann, M. Golling, T. Südmeyer, and U. Keller, "Ultrafast thin-disk laser with 80 μJ pulse energy and 242 W of average power," *Opt. Lett.*, vol. 39, no. 1, p. 9, Jan. 2014, doi: 10.1364/OL.39.000009.

[29] F. X. Kartner, I. D. Jung, and U. Keller, "Soliton mode-locking with saturable absorbers," *IEEE J. Sel. Topics Quantum Electron.*, vol. 2, no. 3, pp. 540–556, Sep. 1996, doi: 10.1109/2944.571754.

[30] R. Paschotta and U. Keller, "Passive mode locking with slow saturable absorbers," *Appl. Phys. B, Lasers Opt.*, vol. 73, no. 7, pp. 653–662, Nov. 2001, doi: 10.1007/s003400100726.

[31] U. Keller, K. J. Weingarten, F. X. Kartner, D. Kopf, B. Braun, I. D. Jung, R. Fluck, C. Honninger, N. Matuschek, and J. A. D. Au, "Semiconductor saturable absorber mirrors (SESAM's) for femtosecond to nanosecond pulse generation in solid-state lasers," *IEEE J. Sel. Topics Quantum Electron.*, vol. 2, no. 3, pp. 435–453, Sep. 1996, doi: 10.1109/2944.571743.

[32] F. Meyer, N. Hekmat, S. Mansourzadeh, F. Fobbe, F. Aslani, M. Hoffmann, and C. J. Saraceno, "Optical rectification of a 100 W average power mode-locked thin-disk oscillator," *Opt. Lett.*, vol. 43, no. 24, p. 5909, Dec. 2018, doi: 10.1364/OL.43.005909.

[33] B. Globisch, R. J. B. Dietz, S. Nellen, T. Göbel, and M. Schell, "Terahertz detectors from be-doped low-temperature grown InGaAs/InAlAs: Interplay of annealing and terahertz performance," *AIP Adv.*, vol. 6, no. 12, Dec. 2016, Art. no. 125011, doi: 10.1063/1.4971843.

[34] W. Withayachumnankul and M. Naftaly, "Fundamentals of measurement in terahertz time-domain spectroscopy," *J. Infr., Millim., THz Waves*, vol. 35, no. 8, pp. 610–637, Aug. 2014, doi: 10.1007/s10762-013-0042-z.

[35] D. Damyanov, A. Batra, B. Friederich, T. Kaiser, T. Schultze, and J. C. Balzer, "High-resolution long-range THz imaging for tunable continuous-wave systems," *IEEE Access*, vol. 8, pp. 151997–152007, 2020, doi: 10.1109/ACCESS.2020.3017821.

[36] S. F. Busch, M. Weidenbach, M. Fey, F. Schäfer, T. Probst, and M. Koch, "Optical properties of 3D printable plastics in the THz regime and their application for 3D printed THz optics," *J. Infr., Millim., THz Waves*, vol. 35, no. 12, pp. 993–997, Dec. 2014, doi: 10.1007/s10762-014-0113-9.

[37] K. Nallappan, Y. Cao, G. Xu, H. Guerboukha, C. Nerguizian, and M. Skorobogatiy, "Dispersion-limited versus power-limited terahertz communication links using solid core subwavelength dielectric fibers," *Photon. Res.*, vol. 8, no. 11, pp. 1757–1775, Nov. 2020, doi: 10.1364/PRJ.396433.

[38] N. Venkatanath, D. Praneeth, M. C. Bh, S. S. Channappayya, and S. S. Medasani, "Blind image quality evaluation using perception based features," in *Proc. 21st Nat. Conf. Commun. (NCC)*, Feb. 2015, pp. 1–6, doi: 10.1109/NCC.2015.7084843.

SAMIRA MANSOURZADEH received the M.S. degree in laser and photonics from Ruhr-Universität Bochum, Germany, in 2018, where she worked on pulse laser compression and characterization. She is currently pursuing the Ph.D. degree, as a Research Assistant, with the Chair of Photonics and Ultrafast Laser Science (PULS).

Since 2018, she has been a part of the "MARIE" project for high-power THz mobile sources and sensing. Her research interests include the ultrafast laser developing, THz generation, detection, and its application in the imaging technology.

DILYAN DAMYANOV received the master's degree in communication engineering from the University of Duisburg–Essen, Germany, in 2014, where he is currently pursuing the Ph.D. degree in electrical engineering.

Since 2014, he has been a Research Assistant with the Chair of Communication Systems, University of Duisburg–Essen. Since 2016, he has been a part of the "MARIE" project for mobile material characterization and localization by electromagnetic sensing using mobile THz systems. His research interests include broadband radar sensors for fire and security applications and especially radar localization, wavefront detection, and imaging techniques.

TIM VOGEL received the B.Sc. and M.Sc. degrees in physics from Heinrich-Heine University, Düsseldorf, Germany. He wrote his bachelor's thesis on the setup of a 3rd order autocorrelator in the Laser Plasma Group, Düsseldorf, and wrote his master's thesis at Airbus Defence & Space, where he characterized a mirror mechanism for the gravitational wave detector LISA. He is currently pursuing the Ph.D. degree in high power THz generation and optimization of THz-time domain spectroscopy.

In 2019, he joined the Photonics and Ultrafast Laser (PULS) Group, Ruhr Universität Bochum.

FRANK WULF received the M.Sc. degree in physics from Friedrich-Schiller-University, Jena, in 2014, where he worked on the generation of near infrared few-cycle pulses and their application to strong-field physics. He is currently pursuing the Ph.D. degree in high power THz generation, driven by mode-locked thin-disk lasers with Ruhr Universität Bochum. He was with the Electrical Engineering Department, Ruhr-University Bochum. In 2014, he moved to the University of Duisburg–Essen, where he was involved in the development of a high-power mid-infrared optical parametric chirped pulse amplification systems.

ROBERT B. KOHLHAAS received the M.Sc. degree in physics from Technische Universität Berlin, Germany, in 2016, where he is currently pursuing the Ph.D. degree in physics, as a graduate student Subsequently, he joined the Fraunhofer Institute for Telecommunications, Heinrich Hertz Institute, Berlin, where he was a Research Associate and a Project Manager.

His research interests include ultrafast photoconductive materials, photoconductive THz antennas, and optoelectronic THz systems.

BJÖRN GLOBISCH studied physics in Aachen, Madrid, and Berlin. He received the Diploma degree in physics from Technische Universität Berlin, Germany, in 2011, and the Ph.D. degree in physics from the University of Marburg, Germany, in 2017. Afterwards, he joined the Fraunhofer Institute for Telecommunications, Heinrich Hertz Institute (HHI), Berlin, Germany as a Research Associate.

Since 2017, he has been the Head of the Terahertz Sensor Systems Group, Fraunhofer, HHI. Since 2019, he has also been an Associate Professor of terahertz sensing with the Institute of Solid-State Physics, Technische Universität Berlin. His research interests include transport and ultrafast phenomena in semiconductors, pulsed and continuous wave terahertz components and systems, and photonic integration.

THORSTEN SCHULTZE received the Diploma degree in electrical engineering from the University of Duisburg–Essen in 2003, and the Ph.D. degree in electrical engineering in 2010.

He is currently as an Academic Senior Councilor (Akademischer Oberrat) with the Chair of Communication Systems, University of Duisburg–Essen. His current research interests include automatic fire detection technologies and broadband microwave, and THz analyses for fire and security applications.

MARTIN HOFFMANN was born in Dessau, Germany, in 1979. He received the Diploma degree in physics and the Ph.D. degree in physics from ETH Zürich, Zürich, Switzerland, in 2007 and 2011, respectively. He was a Researcher with Cyber Laser Inc., Tokyo, Japan, from 2012 to 2013, and a Senior Scientist with the Time and Frequency Laboratory, University of Neuchatel, Neuchatel, Switzerland, from 2013 to 2016.

Since 2016, he has been a Researcher with Ruhr Universität Bochum, Bochum, Germany, where he is currently a Senior Scientist with the Chair of Photonics and Ultrafast Lasers Science.

JAN C. BALZER was born in Unna, Germany, in 1984. He received the Dipl.-Ing. (FH) degree in telecommunications from the University of Applied Science, Dortmund, Germany, in 2008, the M.Sc. degree in electrical engineering and information technology from Ruhr-Universität Bochum, Germany, in 2010, and the Ph.D. degree in electrical engineering, for his work on ultrafast semiconductor lasers, from Ruhr-Universität Bochum, Germany, in 2014.

In 2015, he joined as a Postdoctoral Research Fellow the Group of Prof. Martin Koch, Philipp-Universität Marburg. Since 2017, he has been an Assistant Professor with the Faculty of Engineering, University of Duisburg–Essen, where he combines his knowledge of ultrafast semiconductor lasers with his expertise in system building of THz spectrometers. His current research interest includes THz technology and its application.

CLARA J. SARACENO was born in Argentina, in 1983. She received the Diploma degree in engineering and the M.Sc. degree from the Institut d'Optique Graduate School, Paris, and the Ph.D. degree in physics with ETH Zürich, in 2012. From 2013 to 2014, she was a Postdoctoral Fellow with the University of Neuchatel and ETH Zürich, followed by a postdoctoral position with ETH Zürich, from 2015 to 2016.

In 2016, she received a Sofja Kovalevskaja Award of the Alexander von Humboldt Foundation and became an Associate Professor of photonics and ultrafast science with the Electrical Engineering Faculty, Ruhr Universität Bochum, Germany, where she has been a Full Professor since 2020. Her current research interests include high-power ultrafast lasers and Terahertz science and technology. In 2018, she received an ERC Starting Grant, and in 2019 was selected as an OSA Ambassador. She received the ETH Medal and the European Physical Society (Quantum Electronics and Optics Division) thesis prize in applied aspects for her Ph.D. degree in 2013.